View metadata, citation and similar papers at core.ac.uk

brought to you by CORE

provided by Infoscience - École polytechnique fédérale de Lausanne

OPTIMIZATION OF HIGH EFFICIENCY SILICON HETEROJUNCTION SOLAR CELLS USING SILANE-PLASMA DIAGNOSTICS

A. Descoeudres, L. Barraud, R. Bartlome, P. Bôle Rothen, G. Choong, S. De Wolf, F. Zicarelli and C. Ballif
Ecole Polytechnique Fédérale de Lausanne (EPFL), Institute of Microengineering (IMT),
Photovoltaics and thin film electronics laboratory
Rue A.-L. Breguet 2, CH-2000 Neuchâtel, Switzerland
Phone: +41 32 7183284 ; Fax: +41 32 7183201 ; email: antoine.descoeudres@epfl.ch

ABSTRACT: In silicon heterojunction solar cells, the passivation of the crystalline silicon wafer surfaces and fabrication of emitter and back surface field are all performed by intrinsic and doped amorphous silicon thin layers, usually deposited by plasma-enhanced chemical vapor deposition (PECVD). Since the properties of materials deposited by PEVCD are directly linked to the plasma properties, plasma diagnostics are very useful tools to optimize such devices. A novel diagnostic has been developed to measure *in-situ* the molecular silane depletion fraction in the plasma during deposition. It is found that the silane depletion strongly depends on the process parameters, and appears to be a relevant parameter for the quality of the passivating layers. Good passivation is indeed obtained from highly depleted silane plasmas. Based on this, layers deposited in a large-area PECVD reactor working at very high frequency (40.68 MHz) were optimized for heterojunction solar cells. All other fabrication steps were also fully industry compatible, using sputtering for transparent conductive oxide layers and screen-printing for the front grid. The best 2 x 2 cm^2 cell shows a high open-circuit voltage of 717 mV, yielding a conversion efficiency of 20.3% (aperture area).
Keywords: Heterojunction, PECVD, High-Efficiency

1 INTRODUCTION

Silicon heterojunction solar cells have a high conversion efficiency potential [1-5], up to 23% to date [6]. They are fabricated at low temperatures, and, potentially, at a relatively low-cost. The passivation of the crystalline silicon (c-Si) wafer surfaces is usually performed by very thin intrinsic amorphous silicon (a-Si:H) layers, deposited by RF plasma-enhanced chemical vapor deposition (PECVD) [2, 3, 5] or similar methods (DC PECVD [3], hot-wire CVD [4]). The emitter and the back surface field of the cell are also formed with PECVD doped a-Si:H or doped microcrystalline (μc-Si:H) layers. It has been shown that very thin amorphous silicon layers can provide excellent passivation of crystalline silicon surfaces [7-10]. However, in order to produce high-efficiency devices, it is crucial to control the properties of the intrinsic and doped a-Si:H layers during deposition. This task is usually difficult for heterojunction solar cells, because the layers thicknesses have to be kept very low, in the order of 10 to 15 nm. Consequently, the PECVD processing times are also very short. Since the properties of materials deposited by PEVCD are directly linked to the plasma properties, plasma diagnostics are very useful tools in this context. They give fundamental insights into deposition mechanisms and can be efficiently used for optimization of devices.

Properties of a-Si:H layers have already been studied *in-situ* with optical methods [2, 11]. Here, a novel infrared laser-based plasma diagnostic tool is used in order to measure *in-situ* the silane (SiH_4) density and depletion fraction during deposition of the a-Si:H layers [12]. Silane depletion measurements have already provided useful insights, such as the explanation of the origin of higher deposition rates when using very high frequency (VHF) instead of standard 13.56 MHz [13], the determination of the transition region between amorphous and microcrystalline silicon depositions [14], or the optimization of reactor configurations for fast equilibration after plasma ignition [15]. In this paper, the influence of the silane depletion on a-Si:H layers used for c-Si wafer passivation is studied. A more complete characterization of the plasma properties was obtained by combining these silane depletion measurements with other classical plasma diagnostics. From the results of this passivation study, the a-Si:H layers deposited for heterojunction solar cells were optimized.

2 EXPERIMENTS

Amorphous silicon layers were deposited at 200°C in an automated large-area (electrode size 50 x 60 cm^2), narrow-gap (13 mm), parallel-plate PECVD reactor powered at VHF (40.68 MHz). This reactor is a modified version of an industrial KAI-M PlasmaBox^{TM} reactor [16]. It is equipped with a plasma impedance probe (Z-scan probe from Advanced Energy) located between the matching network and the electrode power feed-in, allowing us to measure the active power P_{ac} defined by

$$P_{ac} = V_{rms} \cdot I_{rms} \cdot \cos\phi \ ,$$

where V_{rms} and I_{rms} are the root mean square values of the VHF excitation voltage and current respectively, and ϕ is the phase between them. Since these measurements are time-resolved, the precise duration of the discharges can be deduced from them. Depending on the discharge regime, plasma polymerization leading to powder formation can occur [17]. The presence of powder can be detected in the gas evacuation line of our reactor by visible laser light scattering (LLS) [18]. Optical emission spectroscopy (OES) completes further the characterization of the plasma properties.

Figure 1 shows schematically the silane depletion measurement setup. The silane depletion D is defined by

$$D = 1 - \frac{n_{SiH4}}{n^0_{SiH4}} \ ,$$

where n^0_{SiH4} is the initial silane density in the reactor before plasma ignition, and n_{SiH4} is the silane density

during the plasma steady state. At constant pressure, a fraction of the silane molecules is dissociated by electron impact in the glow discharge into radicals and hydrogen, leading to a decrease of the initial silane density. The radicals created by dissociation contribute to some extent to the deposition of a-Si:H on the substrate and the reactor walls, the rest is pumped away or leads eventually to the formation of polysilane or powder. The silane densities before and during the discharge are deduced from light absorption measurements (the light absorption is proportional to the density of the absorbing molecules). Silane molecules have many rotovibrational absorption lines in infrared, therefore a light source emitting in this region is required to perform such measurements. In this work a quantum cascade laser (QCL) is used [12, 19], whose wavelength can be tuned between 2241 and 2245 cm^{-1} allowing us to reach much higher resolution than Fourier transform infrared spectroscopy (FTIR). The monochromatic infrared light is focused and injected through the reactor, and the light intensity is measured on the other side. The use of a chopper and a lock-in amplifier improves the diagnostic sensitivity. Measurements of light intensities through the pumped reactor (base vacuum level), through the reactor filled with silane at working pressure before ignition, and through the reactor during the steady-state discharge allow us to deduce the silane depletion *D*.

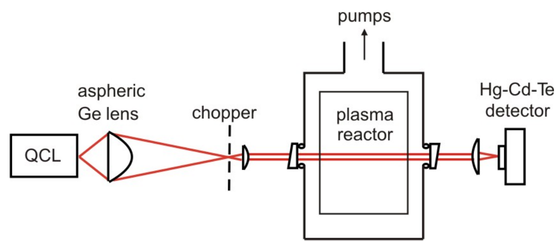

Figure 1: Schematic drawing of the silane depletion measurement setup. The depletion fraction is deduced from infrared light absorption spectroscopic measurements.

For passivation studies presented in this paper, intrinsic a-Si:H layers of about 15-20 nm were deposited on both sides of 300 µm thick *n*-type <100> float zone (FZ) c-Si wafers (4 Ω·cm), using PECVD with pure silane flow plasmas. Just prior to deposition, native oxide on wafer surfaces was removed in an HF solution. Layers were analyzed with spectroscopic ellipsometry. Knowing layer thicknesses and discharge durations, deposition rates can then be estimated. Effective minority carrier lifetimes were measured as deposited and after annealing (180°C for 90 minutes in air) with a Sinton Consulting WCT-100 quasi-steady-state photoconductance system [20].

The structure of the 2 x 2 cm^2 heterojunction solar cells was as follows: Ag front grid / In_2O_3:Sn (ITO) 80 nm / p^+ a-Si:H 10 nm / *i* a-Si:H 5 nm / textured FZ *n* c-Si 300 µm / *i* a-Si:H 5 nm / n^+ a-Si:H 10 nm / ITO 50 nm / Ag back metallization. First, the *n*-type <100> FZ c-Si wafers were textured in KOH and wet-chemically cleaned, and finally dipped in an HF solution just before PECVD in order to remove the native oxide. Intrinsic and doped a-Si:H layers were deposited using mixtures of SiH_4, H_2, PH_3 and $B(CH_3)_3$. Both ITO layers and the back metallization were deposited by DC magnetron sputtering [21]. A front grid was screen-printed with a low temperature silver paste [22]. Finally, the cells were annealed in order to cure the paste. All these fabrication steps are fully compatible for cell production at an industrial scale.

3 RESULTS AND DISCUSSION

3.1 Silane plasma properties and c-Si wafer passivation quality

Figure 2 shows an example of a time-resolved depletion measurement. The initial silane density drops at ignition because the gas is dissociated by the discharge. This increase in the depletion fraction occurs here within the first second of the discharge, but it can be even faster depending on the reactor configuration [15]. A transient phase is then observed during approximately the first 5 seconds, where both active power and depletion are oscillating before stabilizing at a steady-state value. These oscillations are also observed in time-resolved OES acquisitions, for every spectral line (mainly Si, SiH and H_2). The depletion returns slowly to zero as soon as the power is shut down. This decrease in *D* during the afterglow occurs in roughly 10 seconds, the time for the radicals to be pumped away or to recombine.

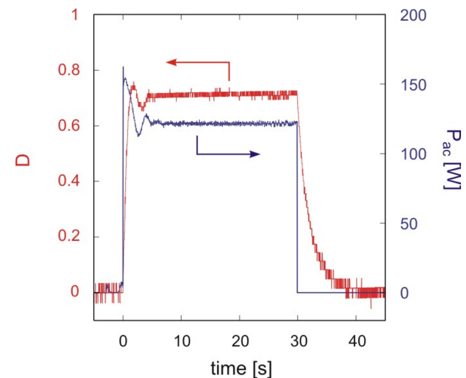

Figure 2: Example of time-resolved measurements of the silane depletion *D* and of the active power P_{ac} (120 sccm SiH_4, 1 mbar, 200 W, 30 seconds discharge, ignition at t=0).

Figure 3 shows the silane depletion fraction *D*, the active power P_{ac} (steady-state values), the deposition rate *R* and the effective minority carrier lifetime τ of the passivated wafers as a function of the three main process parameters, namely the VHF input power, the silane flow and the total pressure (the effect of the deposition temperature was not investigated). Lifetime values are given at a minority carrier density of 10^{15} cm^{-3}. In each panel of figure 3, only one process parameter was varied while the others were kept constant. Data are fitted only for the sake of clarity, and the fits do not have any physical meaning.

It can be seen that the silane depletion *D* depends strongly on the process parameters, going from 0.5 to 0.9 in the range of discharge regimes explored here. *D* increases with the VHF power because the silane dissociation rate is in first approximation proportional to the power, and *D* decreases (increases) with the flow

(pressure) because the SiH_4 residence time in the reactor is decreased (increased) [14].

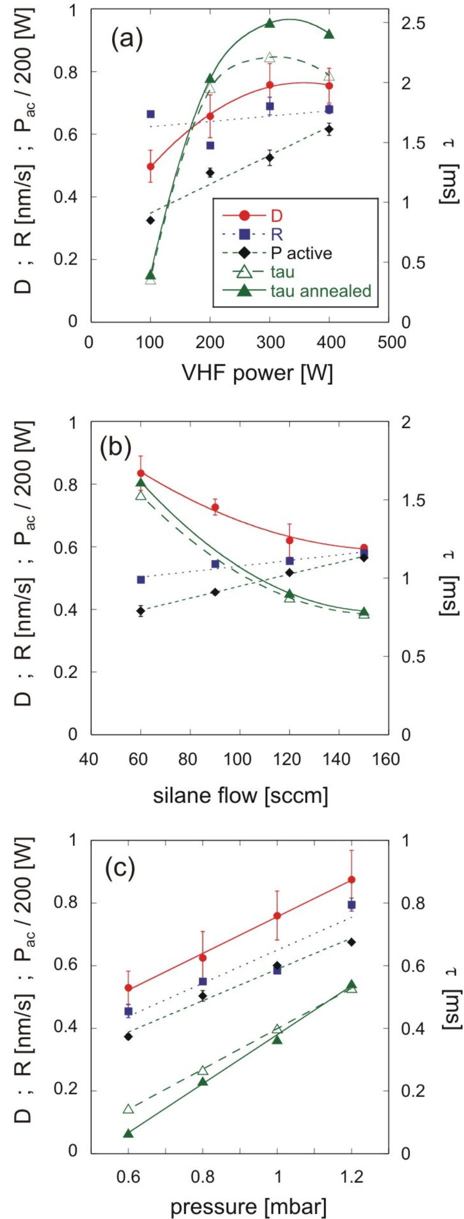

Figure 3: Depletion fraction *D*, deposition rate *R*, active power P_{ac} and minority carrier lifetime τ as a function of (a) the VHF power (120 sccm SiH_4, 0.8 mbar); (b) the silane flow (200 W, 0.8 mbar); (c) the total pressure (200 W, 120 sccm SiH_4). Wafers are passivated with 18 ± 3 nm intrinsic a-Si:H layers and are annealed at 180°C for 90 minutes.

Whereas the deposition rate *R* clearly increases with both the silane flow and the pressure, its behavior as a function of power is less obvious. An increase in *R* with the power could be expected, but in our case it saturates at around 0.7 nm/s above 300 W. This is due to powder formation at this threshold, as confirmed by LLS measurements (not shown). The presence of powders was also clearly seen in time-resolved plasma impedance and OES measurements, with values strongly fluctuating in time, which is a signature of dusty regimes [23].

Interestingly, the minority carrier lifetime τ of as-deposited and annealed passivated wafers follows the same trend as the silane depletion fraction in the power, silane flow, and pressure series. High lifetimes were obtained from highly depleted silane plasmas. In other words, passivation is improved with layers deposited close to microcrystalline regimes [14]. This result can be linked to other silicon thin film solar cell studies, where it is found that the best a-Si:H material quality is reached just before the amorphous-to-microcrystalline transition [24-25]. Thus, contrary to other plasma properties such as the active power or the deposition rate for example, a relevant parameter to characterize the passivating quality of a-Si:H layers deposited from pure silane plasmas appears to be the silane depletion. It is known that the structure of a-Si:H films depends on the plasma properties, mainly through the equilibration of the chemical potential of hydrogen in the plasma and in the film during growth [26]. The a-Si:H/c-Si interface itself is also strongly affected by the hydrogen content and structure of the a-Si:H film [10, 27]. Since hydrogen in the plasma plays such a critical role in the structure of the deposited film, it is clear that the silane depletion can be a physically relevant parameter for assessing the quality of the passivating layers. A detailed description of the link between depletion and passivation through hydrogen chemical reactions is, however, beyond the scope of this paper.

The optimization of passivating layers is thus greatly facilitated and accelerated if one knows the silane depletion, since the three main process parameters can be reduced to only one, which in addition can be measured *in-situ* during deposition. It should be noted that this optimization approach is not limited to pure silane flow plasmas, but can also be applied for a-Si:H layers deposited from H_2-diluted SiH_4 flow plasmas for example.

The presence of powder in the plasma does not seem to be detrimental to the passivation quality, as one might first think. Indeed, lifetimes around 2.5 ms were reached above 300 W (dusty regime) in the power measurement series (figure 3a). It has even been shown elsewhere that µc-Si:H solar cell performances can actually improve when material is deposited in powder-rich regimes [28]. On the other hand, the passivation quality is highly sensitive to the reactor state before deposition (cleanliness, cross contamination, base vacuum level, history of preceding depositions for example). Even with identical process parameters, the fluctuation of the lifetime absolute values can hence be high. Nevertheless, the trends of lifetime as a function of the process parameters presented in figure 3 have been checked several times and are reproducible.

3.2 Optimization of heterojunction solar cells

Based on the results presented in the previous section, carrier lifetimes up to 4.8 ms (5.9 ms after annealing) have been reached with 17 nm thick intrinsic a-Si:H layers on FZ polished wafers (figure 4). This demonstrates that layers deposited at relatively high deposition rates (> 0.6 nm/s) with VHF can provide excellent passivation.

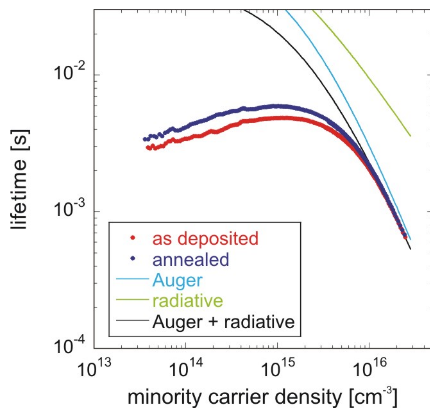

Figure 4: Passivation of a polished FZ wafer with 17 nm thick intrinsic a-Si:H layers (thickness measured by ellipsometry). The Auger and radiative recombination limits are also indicated, for c-Si, *n*-type, 4 Ω·cm.

As shown in figure 5, the best 2 x 2 cm^2 cell obtained with our plasma-based optimization shows a high open-circuit voltage (V_{oc}) of 715 mV, giving a conversion efficiency of 19.9% (aperture area). The addition of a 75 nm thick MgF_2 2nd anti-reflection coating (ARC) on top of the same cell improves mainly the short-circuit current density (J_{sc}), and increases the efficiency up to 20.3%. The highest V_{oc} measured in a cell reaches 720 mV.

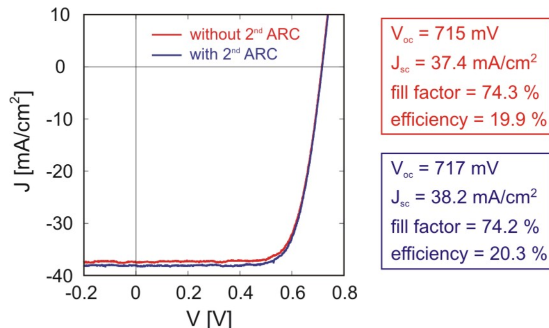

Figure 5: Illuminated IV curve of the best 2 x 2 cm^2 heterojunction solar cell, measured under standard test conditions (in-house measurement).

4 CONCLUSIONS

The use of plasma diagnostics during PECVD is not only useful for a better understanding and control of the process, but it is also highly valuable for the optimization of devices. We have shown that a-Si:H layers used for c-Si wafer passivation can be efficiently tuned knowing the silane depletion fraction during deposition. Indeed, it appears that the depletion is a much more relevant parameter than the power dissipated in the discharge or the deposition rate. In the discharge regimes explored here, good passivating amorphous layers were obtained from highly depleted plasmas, i.e. from regimes closer to microcrystalline regimes.

Layers for silicon heterojunction solar cells have been optimized using this approach. Produced in a large area industrial VHF PECVD reactor, these devices show high open-circuit voltages due to an excellent wafer passivation. The relatively high deposition rates of VHF PECVD are thus perfectly usable in this context. Medium-sized cells with 20% efficiencies have been produced so far, and they will be further optimized and upscaled in the future.

5 ACKNOWLEDGMENTS

The authors would like to acknowledge Dr J. Damon-Lacoste and L. Fesquet for their initial contribution to the work, Y. Andrault for wafer preparation, and Roth & Rau Switzerland for many fruitful discussions.

This work was supported by Axpo AG Switzerland through the Axpo Naturstrom Fond, and by the European Commission through the FP7 project HETSI (Grant No. 211821).

6 REFERENCES

[1] M. Taguchi, K. Kawamoto, S. Tsuge, T. Baba, H. Sakata, M. Morizane, K. Uchihashi, N. Nakamura, S. Kiyama, and O. Oota, Prog. Photovolt: Res. Appl., **8**, 503 (2000).
[2] H. Fujiwara and M. Kondo, J. Appl. Phys., **101**, 054516 (2007).
[3] U. Das, M. Burrows, M. Lu, S. Bowden, and R. Birkmire, Appl. Phys. Let., **92**, 063504 (2008).
[4] Q. Wang, M. Page, E. Iwaniczko, Y. Xu, L. Roybal, R. Bauer, B. To, H.-C. Yuan, A. Duda, F. Hasoon, Y. Yan, D. Levi, D. Meier, H. Branz, and T. Wang, Appl. Phys. Let., **96**, 013507 (2010).
[5] B. Strahm, Y. Andrault, D. Baetzner, D. Lachenal, C. Guérin, M. Kobas, J. Mai, B. Mendes, T. Schulze, G. Wahli, and A. Buechel, Mater. Res. Soc. Symp. Proc., **1245**, A0104 (2010).
[6] M. Taguchi, Y. Tsunomura, H. Inoue, S. Taira, T. Nakashima, T. Baba, H. Sakata, and E. Maruyama, Proceedings of the 24th European Photovoltaic Solar Energy Conference, Hamburg, Germany, 1690 (2009).
[7] J. Pankove and M. Tarng, Appl. Phys. Lett., **34**, 156 (1979).
[8] S. Olibet, E. Vallat-Sauvain, and C. Ballif, Phys. Rev. B, **76**, 035326 (2007).
[9] S. De Wolf and M. Kondo, Appl. Phys. Lett., **90**, 042111 (2007).
[10] S. De Wolf, S. Olibet, and C. Ballif, Appl. Phys. Lett., **93**, 032101 (2008).
[11] J.J.H. Gielis, P.J. van den Oever, M.C.M. van de Sanden, and W.M.M. Kessels, Appl. Phys. Lett., **90**, 202108 (2007).
[12] R. Bartlome, A. Feltrin, and C. Ballif, Appl. Phys. Lett., **94**, 201501 (2009).
[13] L. Sansonnens, A. Howling, and C. Hollenstein, Plasma Sources Sci. Technol., **7**, 114 (1998).
[14] B. Strahm, A. Howling, L. Sansonnens, and C. Hollenstein, Plasma Sources Sci. Technol., **16**, 80 (2007).
[15] A. Howling, B. Strahm, P. Colsters, L. Sansonnens, and C. Hollenstein, Plasma Sources Sci. Technol., **16**, 679 (2007).
[16] J. Perrin, J. Schmitt, C. Hollenstein, A. Howling, and L. Sansonnens, Plasma Phys. Control. Fusion, **42**, B353 (2000).

[17]R. Ross and J. Jaklik, J. Appl. Phys., **55**, 3785 (1984).
[18]R. Roth, K. Spears, G. Stein, and G. Wong, Appl. Phys. Lett., **46**, 253 (1985).
[19]A. Müller and J. Faist, Nature Photonics, **4**, 291 (2010).
[20]R. Sinton and A. Cuevas, Appl. Phys. Lett., **69**, 2510 (1996).
[21]G. Choong, P. Bôle, L. Barraud, F. Zicarelli, A. Descoeudres, S. De Wolf, and C. Ballif, this conference, 2DV.1.25 (2010).
[22]F. Zicarelli, A. Descoeudres, G. Choong, P. Bôle, L. Barraud, S. De Wolf, and C. Ballif, this conference, 2CV.1.74 (2010).
[23]C. Hollenstein, Plasma Phys. Controlled Fusion, **42**, R93 (2000).
[24]G. Yue, D. Han, D. Williamson, J. Yang, K. Lord, and S. Guha, Appl. Phys. Lett., **77**, 3185 (2000).
[25]R. Collins, A. Ferlauto, G. Ferreira, C. Chen, J. Koh, R. Koval, Y. Lee, J. Pearce, and C.Wronski, Sol. Energy Mat. Sol. Cells, **78**, 143 (2003).
[26]R. Street, Phys. Rev. B, **43**, 2454 (1991).
[27]T. Schulze, H. Beushausen, C. Leendertz, A. Dobrich, B. Rech, and L. Korte, Appl. Phys. Lett., **96**, 252102 (2010).
[28]G. Parascandolo, R. Bartlome, G. Bugnon, T. Soederstroem, B. Strahm, A. Feltrin, and C. Ballif, Appl. Phys. Lett., **96**, 233508 (2010).